Chin. J. Astron. Astrophys. Vol. 1, No. 2, (2001) 152–160
(*http://www.chjaa.org* or *http://chjaa.bao.ac.cn*)

Chinese Journal of
Astronomy and
Astrophysics

A Further Study of Relative Longitude Shift of Pulsar Beams

Ren-Xin Xu⋆, Jian-Wen Xu and Guo-Jun Qiao

CAS-PKU Joint Beijing Astrophysical Center and Department of Astronomy, Peking University, Beijing 100871

Received 2001 January 3 ; accepted 2001 February 28

Abstract It is of great importance to study pulsar beam shape if we are concerned with emission theories and pulsar birth rate. Both observations and the ICS model show that different emission components are emitted from different heights. The relative longitude phase shifts due to different heights of the emission components and the toroidal velocity of the electrons are considered in this paper. Several possible observational effects arising from the phase shift are presented. The emission beams may not have circular cross section although the emission region may be symmetric with respect to the magnetic axis.

Key words: pulsars – polarization – radiation mechanisms

1 INTRODUCTION

Soon after the discovery of pulsars, the rotating vector model (RVM) was proposed, which well explained the linear polarization characteristics of pulsar radio emission. In this model Radhakrishnan and Cooke (Radhakrishnan & Cooke 1969) assumed that relativistic particles stream out along dipolar magnetic fields of the pulsar and the polarization position angle of emitted radiation from these particles is correlated with the magnetic curvature. Theoretical extensions of the RVM have appeared in the literature (e.g., Ferguson 1976; Blaskiewicz et al. 1991; Hibschman & Arons 2001), that included some specific physical factors, such as the special relativistic effects and the polar-cap current flow.

However, the RVM fails to explain the jumps in position angle observed in the mean pulse as well as in the individual pulses (Stinebring et al. 1984). This led to the assumption that the pulsar radio beam contains two nearly orthogonal polarization modes, the superposition of which results in the non-S-shaped position angle variation in the mean pulse and the two $\sim 90^\circ$ separated distributions of position angles in individual pulses (see the paper by Mckinnon & Stinebring (1998) and references therein). Nevertheless, there is still a possibility that a modified RVM, *without* the inclusion of the orthogonal modes, can reproduce the observed position angle "jumps" if we take into account the linear depolarization of pulsar beams and the observational uncertainties due to the polarimeters used (Xu, Qiao & Han 1997; Xu & Qiao 2000).

⋆ E-mail: rxxu@bac.pku.edu.cn

In view of the observational fact that the radio emission of pulsars may have three components (core and two cones) which are emitted from different heights above the pulsar surface (Rankin 1983), Xu et al. (Xu, Qiao & Han 1997) found that the position angle of the mean pulse jumps at certain longitudes where the linear polarization is approximately zero if the retardation effect, which causes the beam centers to be shifted relative to one other, leads significantly to linear depolarization.

In this paper, we further study the issue arising from different emission heights calculated according to the inverse Compton scattering model (Qiao & Lin 1998), that naturally reproduce the core and conal components.

Besides the polarization effect discussed above, different emission heights may also have notable consequences on the beam shape. Many authors have investigated observationally the pulsar beam shape, their results are summarized as follows. Jones (1980) finds that the latitudinal radius of beam cross Section could be 2.5 times the longitudinal one. Narayan & Vivekanand (Narayan 1983) modify this ratio to be 3.0. Lyne & Manchester's (Lyne & Manchester 1988) conclusion is that the shape of the emission beam is approximately circular. Biggs (Biggs 1990) proposes that there may be some meridional compression. Wu & Shen (Wu, Shen 1988) find that, for pulsars with short periods, the radius of the emission beam in the latitudinal direction is larger. However, the latitudinal radius is smaller for pulsars with longer periods. Rankin, therefore, changes her morphological beam shape from an elliptical cross section (Rankin 1983) to a circular one (Rankin 1993). Our numerical results in Section 3 may be checked against such observational studies in the future.

We find that the emission beams of pulsars with small rotation periods do not have circular cross sections even if the emission regions are symmetric with respect to the magnetic axis when we take into account the toroidal velocity due to rotation.

This paper is organized as follows. After inspecting various aspects of the retardation effect caused by different emission heights and their possible observational consequences in Section 2, we calculate the emission beam arising from relativistic particles with poloidal (along magnetic field lines) and toroidal (perpendicular to field lines) velocities in Section 3. And it is summarized in Section 4. A statement which gives the phase shift between two emission units at arbitrary positions is proved geometrically in the Appendix.

2 RELATIVE LONGITUDE SHIFT DUE TO DIFFERENT HEIGHTS

It is generally believed that pulsar radio emission originates in the region near the last open field lines. In this section, we assume that the particles in the last-open-field-line region responsible for the observed radiation have only poloidal velocities along the field lines (i.e., the toroidal velocity is neglected), and are accelerated symmetrically relative to the magnetic axis. The emission region of each beam component is thus also symmetric relative to the axis. According to the Appendix, the phase shift of all the emission elements of a given beam component is the same since the values $\boldsymbol{r} \cdot \boldsymbol{n}_0$ of these emission elements is the same, $\boldsymbol{r}$ being the vector position of the element and $\boldsymbol{n}_0$ the emission direction. Therefore the emission beam should have circular cross sections in this case.

2.1 Emission Heights and Beam Shift

We know from the Appendix that an emission element at the vector position $\boldsymbol{r}$ is equivalent to an original virtual one whose longitude phase shifts to an earlier value $\delta\phi(r) = \Omega \boldsymbol{r} \cdot \boldsymbol{n}_0/c$.

We now calculate $\delta\phi(r)$ as a function of r, based on the dipole geometry of magnetic field configuration.

For a dipole field line, we have

$$r = \lambda \frac{cP}{2\pi} \sin^2 \Theta, \tag{1}$$

where $r = |\boldsymbol{r}|$, Θ is the polar angle, P the rotation period, c the speed of light, and λ a parameter which characterizes the sort of field lines ($\lambda \geq 1$, $\lambda = 1$ for the last open field lines). Based on Eq.(1), the angle Θ_μ between the direction of the magnetic field at vector position $\boldsymbol{r}$ and the magnetic axis $\boldsymbol{\mu}$ reads,

$$\begin{aligned} \cos\Theta_\mu &= \frac{2\lambda cP - 6\pi r}{\sqrt{\lambda cP(4\lambda cP - 6\pi r)}}, \\ &= \frac{2 - 3\sin^2\Theta}{\sqrt{4 - 3\sin^2\Theta}}. \end{aligned} \tag{2}$$

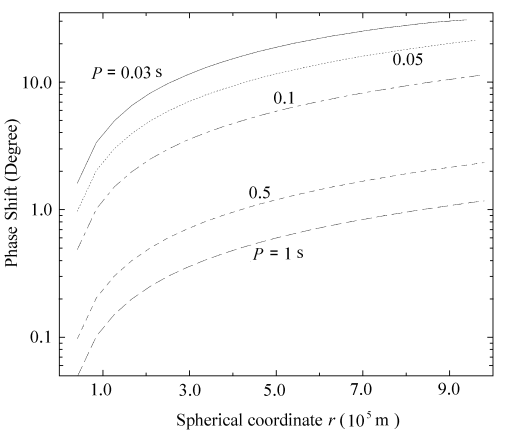

Fig. 1 The phase shift $\delta\phi$ for pulsars with $P = 0.03$, 0.05, 0.1, 0.5, 1.0 s, based on Eq.(3). The emission height (spherical coordinate r) is from 30 to 10^3 km. $\lambda = 1$.

Therefore, assuming that the elementary emission is along the magnetic field lines, according to Eqs.(1)–(2) and the Appendix, we obtain the phase shift $\delta\phi$ as a function of r,

$$\delta\phi(r) = \frac{4\pi r}{\lambda cP} \sqrt{\frac{\lambda cP - 2\pi r}{4\lambda cP - 6\pi r}}, \tag{3}$$

and the phase difference $\Delta\phi$ between two emission beam components of heights r_a and r_b is

$$\Delta\phi = \delta\phi(r_\mathrm{a}) - \delta\phi(r_\mathrm{b}). \tag{4}$$

We note, from Eq.(3), that $\delta\phi$ is a function of the rotation period P and of the distance r, but independent of the magnetic inclination angle α or the impact angle β. The calculation of the phase shift $\delta\phi$ for pulsars with periods $P = 0.03$, 0.05, 0.1, 0.5 and 1.0 s are shown in Fig. 1.

We see also from Fig. 1 that the retardation effect arising from different emission heights is less important for pulsars with longer periods P, but is not negligible when P is small. For instance, the phase difference between the components at heights 30 km and 300 km could be over 10° if $P = 30$ ms. while it is only about 1° for emission components at heights 50 km and 500 km if $P = 0.5$ s.

2.2 The Relationship between the Observing Frequency and Phase Shift

Theoretically, we know the emission heights of beam components at a given observing frequency in the inverse Compton scattering model (Qiao & Lin 1998; Xu et al. 2000), in terms of which the three components (core, inner cone, and outer cone) can be understood naturally. The frequency ν of radio wave emitted at position r (or at height $r - R$, R being the pulsar radius) can be obtained by following Eqs.(5)–(7). Low frequency electromagnetic waves with frequency ν_0 are supposed to be produced near the pulsar surface due to the RS-type vacuum gap sparking (Ruderman & Sutherland 1975). These waves are assumed to propagate nearly freely in the highly inhomogeneous plasma of the pulsar magnetosphere and to be inverse

Compton scattered by the secondary particles with Lorentz factor γ to turn into radio waves observed at frequency ν (Xu et al. 2000),

$$\nu = 1.5\gamma^2\nu_0(1 - \sqrt{1-\gamma^{-2}}\cos\theta_{\rm i}), \tag{5}$$

where the incident angle $\theta_{\rm i}$ is the angle between the wave vector of the low frequency wave and the direction of the electron (moving along the magnetic field in the approximation of this paper), which can be calculated to be

$$\cos\theta_{\rm i} = \frac{2\cos\Theta + (R/r)(1-3\cos^2\Theta)}{\sqrt{(1+3\cos^2\Theta)[1-2(R/r)\cos\Theta+(R/r)^2]}}. \tag{6}$$

The Lorentz factor of the relativistic electron should decrease[1] with height, in the form suggested in (Qiao & Lin 1998):

$$\gamma = \gamma_0 \exp[-\xi\frac{r-R}{R}], \tag{7}$$

where γ_0 is the initial Lorentz factor near the pulsar surface, ξ the parameter reflecting the extent of the energy loss.

The relation between the observing frequency ν and position r can be found from Eqs.(1), (5)–(7). For a given ν we find three solutions for r: r_1, r_2, r_3, the positions of the core, the inner cone, and the outer cone, respectively. The phase differences of the beam components between the outer and inner cones, and between the inner cone and core, are calculated for observing frequencies up to a few GHz in the ICS model; these are shown in Fig. 2.

We see from Fig. 2 that, on one hand, at lower frequencies ν, the phase difference $\Delta\phi_2 \equiv \delta\phi(r_3) - \delta\phi(r_2)$ between the outer and inner cones is notable. For example, $\Delta\phi_2 = 30^\circ$ when $\nu = 2\times10^7$ Hz. And $\Delta\phi_2$ decreases monotonically with increasing ν. On the other hand, the phase difference $\Delta\phi_1 \equiv \delta\phi(r_2) - \delta\phi(r_1)$ between the core and the inner cone components is small at lower ν. $\Delta\phi_1 = 0.05^\circ$ and increases monotonically with increasing ν. The observational tests and/or consequences of these features need further investigation.

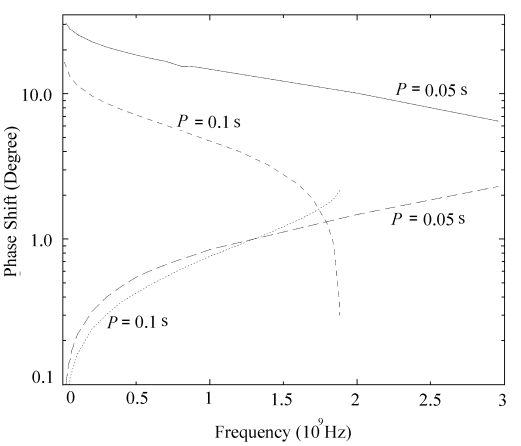

Fig. 2 The phase difference between the beam components as functions of observing frequency for the ICS model. The upper two lines (solid and short dashed) are for the phase difference between the outer and inner cones, while the other lines, between the inner cone and the core. The pulsar periods are chosen to be 0.1 and 0.05 s, and other parameters are $\gamma_0 = 3\times10^3$, $\xi = 3\times10^{-2}$, $R = 10^4$ m, and $\nu_0 = 10^5$Hz. $\lambda = 1$.

[1] Electrons will lose their kinetic energy, via, e.g., curvature radiation and/or the inverse Compton scattering of these electrons off thermal X-ray photons from the pulsar surface, when they are moving along magnetic field lines.

2.3 Possible Distribution of Singular Points on the Celestial Sphere

There may be some points on the celestial sphere where the linear polarization intensity $L = 0$. We call such points "singular points". The polarization position angle should jump[2] by exactly 90° when a line of sight goes across one of the singular points (Xu, Qiao & Han 1997; Xu & Qiao 2000). Therefore the distribution of the singular points on the celestial sphere would determine the properties of the variation in the position angle.

Generally, it is hard to calculate the singular point distribution since there are many factors that are not well understood, that cause depolarization (Xu & Qiao 2000; Lyutikov 1999) of pulsar beamed radiation. However, if the depolarization is mainly due to incoherent superposition of emission components at different heights, and if there are only two components, we may get the singular point distribution easily.

In this special case the sufficient *and* necessary conditions that must be satisfied at a singular point are

$$\begin{cases} \psi_1 - \psi_2 = \pm\pi/2 \\ L_1 = L_2 \end{cases}, \tag{8}$$

where $\psi_{\rm i}$ and $L_{\rm i}$ (i = 1, 2 for the first and second components) are the position angle and linear polarization intensity of the i-th component. The first condition, i.e., $\psi_1 - \psi_2 = \pm\pi/2$, is thus only a *necessary* one for a singular point. Considering the identity $\tan(\psi_1 - \psi_2) = \frac{\tan\psi_1 - \tan\psi_2}{1+\tan\psi_1\tan\psi_2}$, we can rewrite the necessary condition as

$$\tan\psi_1 \tan\psi_2 = -1. \tag{9}$$

The possible distribution of singular points on the celestial sphere is calculated for this special case based on Eq.(9), and shown in Fig. 3. We assume the phase difference between the centers of the components due to their different emission heights to be $\Delta\phi = 15°$, and the inclination angle $\alpha = 60°$ or 30°. We find from Fig. 3 that the distribution become "flatter" when the inclination angle α is smaller, i.e., larger α may be more favorable for a line of sight to go across a singular point, and the possibility of the position angle curve "jumping" is increased.

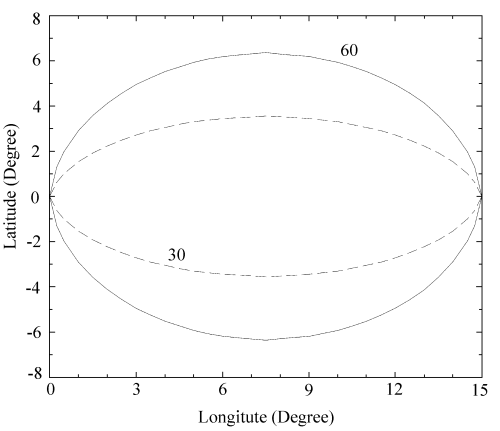

Fig. 3 A possible distribution of singular points on the celestial sphere assuming that there are only two emission components, and that the linear depolarization arises only from the incoherent superposition of those two components. The phase difference between the components is assumed to be 15°, and the inclination angles are chosen to be 30° and 60°, respectively, in the computation.

3 EMISSION BEAMS IN THE ICS MODEL

In the above discussion, only the electron velocity along magnetic field lines (the poloidal velocity) is considered. However, as a pulsar rotates, an electron does have a *toroidal* velocity $\boldsymbol{\Omega} \times \boldsymbol{r}$ (see Fig. 4). Actually, the velocity of an electron in the observer's rest frame can be

[2] The position angle may jump approximately 90° if a line of sight passes near a singular point.

obtained by the relativistic velocity transformation of the poloidal velocity in the rotating frame. The inclusion of the toroidal velocity has at least one implication: an emission unit will undergo a phase shift with respect to the magnetic direction $\boldsymbol{n}_{\rm B}$ since a relativistic electron emits photons in the direction of its motion. In this section, we calculate the beam shape as modified by the inclusion the toroidal velocity, based on the derived emission heights in the ICS model (Qiao & Lin 1998). In the following computation, two phase shift effects, one from different emission heights and one from toroidal velocity are included. According to Fig. 4, one can find the relationship between $\{\theta, \phi\}$ and $\{\Theta, \Phi\}$,

$$\begin{cases} \cos\theta &= \cos\alpha\cos\Theta - \sin\alpha\sin\Theta\sin\Phi \\ \sin\phi &= \dfrac{\cos\alpha\sin\Phi\sin\Theta + \sin\alpha\cos\Theta}{\sin\theta} \\ \cos\phi &= \dfrac{\cos\Phi\sin\Theta}{\sin\theta} \end{cases}, \tag{10}$$

which will prove useful below.

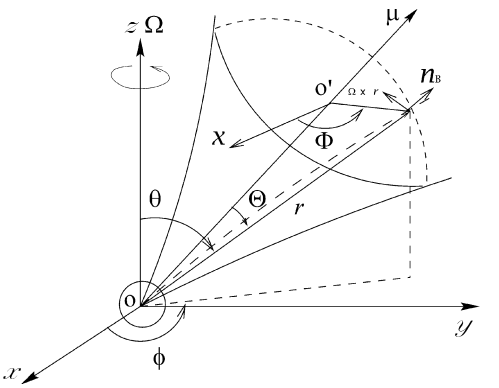

Fig. 4 A sketch of two coordinate systems. we assume the μ-coordinate, in which the magnetic axis μ is chosen as the z-axis, turns clockwise through an angle α (the inclination angle) along the x-axis of the Ω-coordinate. A position vector $\boldsymbol{r}$ can be represented by $\{r, \theta, \phi\}$ in the Ω-coordinate system, or by $\{r, \Theta, \Phi\}$ in the μ-coordinate system. $\boldsymbol{n}_{\rm B}$ is the unit vector of the magnetic field.

We note the linear rotation velocity at a position vector $\boldsymbol{r}$ is v,

$$\begin{aligned} v &= |\boldsymbol{\Omega}\times\boldsymbol{r}| \\ &= \Omega r\sqrt{1-(\cos\alpha\cos\Theta - \sin\alpha\sin\Theta\sin\Phi)^2}\,. \end{aligned} \tag{11}$$

Thus, by the relativistic velocity transformation, one finds two components, u_1 (in the $\boldsymbol{\Omega}\times\boldsymbol{r}$ direction) and u_2 (in the $[(\boldsymbol{\Omega}\times\boldsymbol{r})\times\boldsymbol{n_B}]\times(\boldsymbol{\Omega}\times\boldsymbol{r})$ direction), of the velocity of an electron in the observer's rest frame,

$$\begin{aligned} u_1 &= \frac{-c\sqrt{1-\gamma^{-2}}\sin\alpha\sin\Theta\cos\Phi + v\sqrt{1+3\cos^2\Theta}}{\sqrt{1+3\cos^2\Theta} - v\sqrt{1-\gamma^{-2}}\sin\alpha\sin\Theta\cos\Phi/c}, \\ u_2 &= \frac{c\sqrt{(1-\gamma^{-2})(1-v^2/c^2)(1+3\cos^2\Theta - \sin^2\alpha\sin^2\Theta\cos^2\Phi)}}{\sqrt{1+3\cos^2\Theta} - v\sqrt{1-\gamma^{-2}}\sin\alpha\sin\Theta\cos\Phi/c}, \end{aligned} \tag{12}$$

where γ is the Lorentz factor of the electron in the rotating frame. Therefore the angle δ between $\boldsymbol{n}_{\rm B}$ and the emitted photon is,

$$\delta\varphi = \cos^{-1}\left[\frac{-\sin\alpha\sin\Theta\cos\Theta}{\sqrt{1+3\cos^2\Theta}}\right] - \cos^{-1}\left[\frac{u_1}{\sqrt{u_1^2+u_2^2}}\right], \tag{13}$$

which is also the phase shift due to the toroidal velocity.

Combining the phase shifts of $\delta\phi$ (Eq.(3)) and $\delta\varphi$ (Eq.(13)), we can calculate the emission beams in the ICS model. We use the results in Fig. 2 to clarify the emission heights. The radio emission is assumed to come from a region between magnetic field lines specified by $\lambda = 1.0$ and by $\lambda = 1.8$. The radius of the stellar surface of the feet of the field lines corresponding to $\lambda = 1.8$ is $\sim \lambda^{-1/2}\theta_{\rm p} \sim 0.75\theta_{\rm p}$, where $\theta_{\rm p} = \arcsin\sqrt{\frac{2\pi R}{cP}}$, is the radius of the polar cap. The cases of rotation period $P = 0.1$ and 0.05 s, and observing frequency $\nu = 10^9$ Hz are presented in Fig. 5 and Fig. 6 respectively. The parameters in the simulation are listed in Table 1.

Table 1 The Chosen and Calculated Parameters* in the ICS Model for the Computation of Emission Beam Components

P (s)	ν (Hz)	r_1(m)	r_2 (m)	r_3 (m)	$\theta_{\mu 1}$ (°)	$\theta_{\mu 2}$ (°)	$\theta_{\mu 3}$ (°)	$\Delta\phi_1$ (°)	$\Delta\phi_2$ (°)
0.1	10^9	18820	81900	483820	5.4	11.3	28.1	0.76	4.74
0.05	10^9	20695	56040	697000	8.0	13.2	50.5	0.85	14.71

*P – rotation period; ν – the observing frequency; $r_{\rm i}$ – emission height of component i; $i = 1, 2, 3$ denotes core, inner cone, and outer cone, respectively; $\theta_{\mu{\rm i}}$ – angular radius of component i; $\Delta\phi_1$ and $\Delta\phi_2$ are the phase differences between core and inner cone, and between inner and outer cones, respectively.

From Fig. 5 and Fig. 6, we see that the emission beams are clearly not symmetric, although the emission regions of these components may be symmetric with respect to the magnetic axes. The width of the first pulse in a conal component would be much smaller than that of the second. Besides the clear phase shifts between the components, the emission beams may not have circular cross sections when the rotation period is small (see Fig. 6). The pulses of impact angle $\beta > 0$ arrive earlier than those of $\beta < 0$. This is understandable. Since the emission region of $\beta > 0$ is farther from the rotation axis than that of $\beta < 0$, the phase shift effect here is greater due to a larger toroidal velocity.

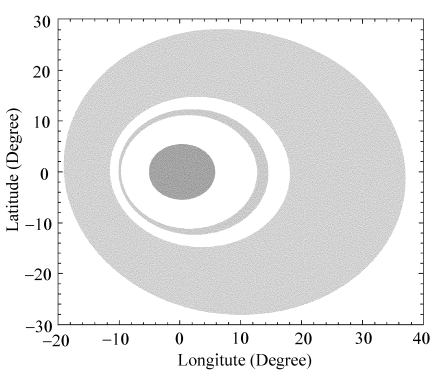

Fig. 5 The emission beams of core, inner cone, and outer cone simulated in the ICS model, with the inclusion of the phase shift effects both due to different emission heights and toroidal velocity. The inclination angle $\alpha = 30°$, the rotation period $P = 0.1$ s. Other parameters are the same as in Fig. 2.

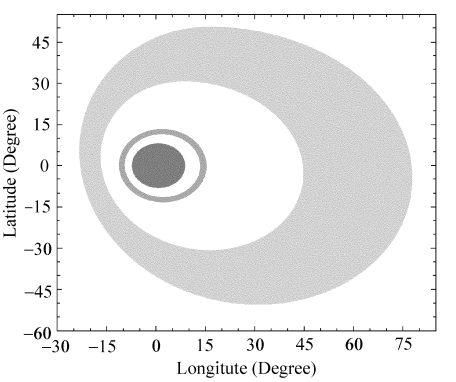

Fig. 6 Same as in Fig. 5, but for $P = 0.05$ s.

4 CONCLUSIONS AND DISCUSSION

A detail consideration of the relative longitude phase shift due to different emission heights of the three components is presented. The main conclusion can be summarized as follows.

(1) An emission unit along the direction $\boldsymbol{n}_1(\theta_0, \phi_1)$ at an arbitrary position $\boldsymbol{r}_1$ arrives

earlier than another emission unit along the direction $\boldsymbol{n}_2(\theta_0, \phi_2)$ at another position $\boldsymbol{r}_2$, the phase difference between these two is $\phi_1 - \phi_2 + \Omega(\boldsymbol{n}_1 \cdot \boldsymbol{r}_1 - \boldsymbol{n}_2 \cdot \boldsymbol{r}_2)/c$ (*if* this value is positive), where Ω is the rotational angular velocity.

(2) The phase shift effect is less important when the rotation period $P > 0.5\,\mathrm{s}$.

(3) The phase shifts, as functions of the observing frequency ν for the ICS model, are presented. As ν increases, the shift between the outer and inner cones decreases, while the shift between the inner cone and core increases.

(4) Larger inclination angles are more favorable for the appearance of jumps in the polarization position angle.

(5) The emission beams are not symmetric in the ICS model, when the phase shift effects due to both different emission heights and toroidal velocity ($\boldsymbol{\Omega} \times \boldsymbol{r}$) are included.

In the simulation of the beam shape, we just took the symmetric emission region in the ICS model for simplicity. However, the emission region should actually *not* be symmetric with respect to the magnetic axes, when we consider that, for a given inverse Compton scattering process, the low-frequency wave is emitted at an earlier sparking point, and that electrons are not moving exactly along magnetic field lines. How about the emission beams and polarization properties when these considerations are included? A further study is called for.

Appendix

Observations show that emission components (core, inner cone, and outer cone) could come from different heights (Rankin 1983). The longitude phase shifts between these components are thus inevitable (Xu, Qiao & Han 1997). We now try to evaluate this shift between two emission components. We procedure is as follows. First, we find a virtual equivalent[3] at origin for an emission unit at arbitrary position; then we compare the phases of the virtual equivalents. The phase difference between two virtual equivalents is actually the observed phase difference of those two corresponding emission units. Our conclusion can be expressed as the following proposition:

An emission unit along a direction $\boldsymbol{n}_0(\theta_0, \phi_0)$ at an arbitrary position $\boldsymbol{r}(\theta, \phi)$ is equivalent observationally to a virtual emission unit along the direction $\boldsymbol{n}'_0(\theta_0, \phi'_0)$ at origin, where $\phi'_0 = \phi_0 + \Omega\tau$, $\tau = \boldsymbol{r} \cdot \boldsymbol{n}_0/c$, Ω and c are the rotational angular velocity and the speed of light, respectively.

Our proof now follows. Referring to Fig. 7, we erect coordinates $o - xyz$ in the observer's rest frame, where z-axis is along the rotational axis ($\boldsymbol{\Omega}$), the origin is at the center of the pulsar. We consider the emission along $\boldsymbol{n}_0$ at an arbitrary point E. A plane ABC is created so that $\boldsymbol{n}_0$ is perpendicular to it. Because all of the emission units along the direction $\boldsymbol{n}_0$ at those points which are on the ABC plane should be observed simultaneously, the emission along $\boldsymbol{n}_0$ at point F[4], F is equivalent to the emission at point E if the intensities are the same. We assume the time $t = 0$ when a photon is emitted at point E along $\boldsymbol{n}_0$. A photon emitted at point O along $\boldsymbol{n}_0$ when $t = -\tau$ ($\tau = |\boldsymbol{OF}|/c$) arrives at point F when $t = 0$ (still along $\boldsymbol{n}_0$). However, at $t = 0$, the emission at point O is along $\boldsymbol{n}'_0(\theta_0, \phi_0 + \Omega\tau)$ because of the rotation. Therefore, an emission along $\boldsymbol{n}_0$ at point E with position vector $\boldsymbol{r}$ is equivalent to the virtual one along $\boldsymbol{n}'_0$ at origin O. Then we calculate the value τ. In the right-angled triangle OEF, $|\boldsymbol{OF}| = \boldsymbol{r} \cdot \boldsymbol{n}_0$. We thus have $\tau = \boldsymbol{r} \cdot \boldsymbol{n}_0/c$.

[3] We call two emission units equivalent if an observer at infinity can not distinguish them, i.e., the observer detects the same intensity at same time for those two emission units.

[4] Point F is the intersection of plane ABC and its perpendicular line through point O.

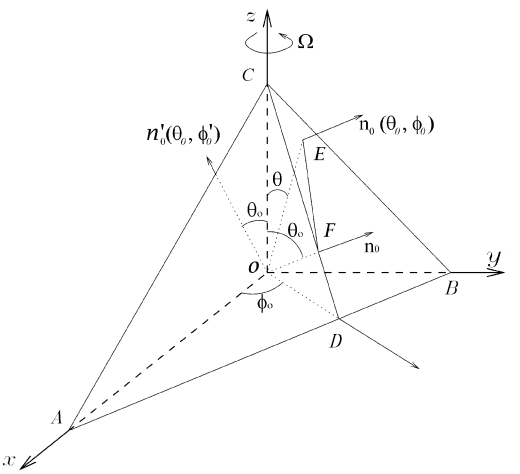

Fig. 7 A sketch illustrating the geometry involved in our proposition that an emission along $\boldsymbol{n}_0$ at point E (position vector $\boldsymbol{r}$) is equivalent to a virtual emission along $\boldsymbol{n}'_0$ at the origin.

Acknowledgements We thank our pulsar group for discussions. This work is supported by NSFC (No. 19803001), by the Special Funds for Major State Basic Research Project, and by Doctoral Program Foundation of Institution of Higher Education in China.

References

Biggs J. D., 1990, MNRAS, 245, 514
Blaskiewicz M., Cordes J. M., Wasserman I., 1991, ApJ, 307, 643
Ferguson D. C., 1976, ApJ, 205, 247
Hibschman J. A., Arons J., 2001, ApJ, in press (astro-ph/0008117)
Jones P. B., 1980, ApJ, 236, 661
Lyne A. G., Manchester R. N., 1988, MNRAS, 234, 477
Lyutikov M., 1999, ApJ, 525, L37
Mckinnon M. M., Stinebring D. R., 1998, ApJ, 502, 883
Narayan R., Vivekanand M., 1983, A&A, 122, 45
Qiao G. J., Lin W. P., 1998, A&A, 333, 172
Radhakrishnan V., Cooke D. J., 1969, ApJ, 3, L225
Rankin J. M., 1983, ApJ, 274, 333
Rankin J. M., 1993, ApJ, 405, 285
Ruderman M. A., Sutherland P. G., 1975, ApJ, 196, 51
Stinebring D. R. et al., 1984, ApJS, 55, 247
Wu X. J., Shen J. X., 1988, Kexue Tongbao, 20, 1567 (in Chinese)
Xu R. X., Qiao G. J., Han J. L., 1997, A&A, 323, 395
Xu R. X., Qiao G. J., 2000, Science in China, A43, 439
Xu R. X., Liu J. F., Han J. L., Qiao G. J., 2000, ApJ, 535, 354